Polarimetric Matched Filtering for Distributed Scatterers

J. G. Teti, Jr.[†], J. S. Verdi, W.-M. Boerner[‡]

[†]Lambda Science, Inc.
P.O. Box 238
Wayne, PA 19087-0238, USA

[‡]University of Illinois at Chicago, EECS
Communications, Sensing & Navigation Lab, M/C
Chicago, IL 60607-7018,USA

Naval Air Warfare Center
Aircraft Division
Warminster, PA 18974-0591, USA

Abstract - The theory for polarimetric matched filter processing has been primarily developed for point scatterers. However, complex scatterers of interest (either man-made or natural) are distributed scatterers consisting of multiple scattering centers. Many modern polarimetric radar systems have the resolution performance to resolve the multiple scattering centers that together comprise an individual distributed scatterer return. The individual scattering centers of a distributed scatterer can often exhibit different polarimetric characteristics, and consequently do not reliably respond to polarimetric matched filter processing techniques that have been derived for individual point scatterers. This paper presents a matched filter processing technique that treats distributed scatterers explicitly. The technique is applicable to any high resolution polarimetric radar, but improved polarimetric processing for synthetic aperture radar (SAR) imagery is the motivation for its development. The technique is described and demonstrated using simulated SAR data for the simple case of a distributed scatterer consisting of linear orthogonal co-pol (HH and VV) scattering centers.

Introduction

Many modern polarimetric sensors have the resolution performance to resolve multiple scattering centers that together comprise a distributed scattering signature. A distributed scatterer can often contain multiple polarimetric scattering characteristics, and consequently are difficult to enhance with polarimetric processing techniques derived for individual point scatterers. An approach to polarimetric matched filtering for distributed scatterers is presented that is formulated as an extension of the results derived for point scatterers. Consider the polarization state of the transmitted or incident wave given by

$$\bar{E}_i = \left(E_{iH}(x,y)\hat{e}_x + E_{iV}(x,y)\hat{e}_y\right) e^{j(2\pi ft \pm kz)} \qquad (1)$$

where the widely accepted definitions for notation apply. The horizontal and vertical components of the incident electric field are given by

$$\begin{bmatrix} E_{iH} \\ E_{iV} \end{bmatrix} = \begin{bmatrix} a_H \cos(\alpha) \\ a_V \sin(\alpha) e^{j\beta} \end{bmatrix} \qquad (2)$$

where the angles α and β are related to the orientation ψ and ellipticity χ angles by $\cos(2\alpha) = \cos(2\psi)\cos(2\chi)$ and $\tan(\beta) = \tan(2\chi)/\sin(2\psi)$. The energy density (power) in the scattered field is given by

$$P_s = \bar{E}_s^\dagger \bar{E}_s = \bar{E}_i^\dagger S^\dagger S \bar{E}_i = \bar{E}_i^\dagger G \bar{E}_i \qquad (3)$$

where $G = S^\dagger S$ is the Hermitian Graves power matrix [1-3]. The formulation of the polarimetric matched filter (PMF) and its more generalized extension to contrast enhancement is based on the maximization of (3). Explicitly, consider two different regions in an image denoted by A and B, where it is desirable to enhance the detection of A in the presence of B. Note that for this work A is a distributed scatterer to be detected and B could represent clutter. For the case of point scatterers, the associated scattering matrices can be used with (3) to match the polarization state of the incident field to maximize the power in the scattered field. The quantity to maximize is the Rayleigh quotient given by

$$\Omega = \frac{P_s^A}{P_s^B} = \frac{\bar{E}_i^\dagger G_A \bar{E}_i}{\bar{E}_i^\dagger G_B \bar{E}_i}, \qquad (4)$$

as suggested in [3]. Maximizing Ω reduces to solving the generalized eigenvalue problem [4]

$$G_A \bar{E}_i^{opt} = \lambda G_B \bar{E}_i^{opt}. \qquad (5)$$

Note that for $G_B = I$, the identity matrix, (4) corresponds to the basic PMF formulation. In either case, the quantity $0 \le (\lambda_2 - \lambda_1)/(\lambda_1 + \lambda_2) \le 1$ indicates the separation extremes that can be observed between the characteristic polarization signatures of A and B. The optimum polarization state $\bar{E}_i^{opt}$ $(= \bar{E}_{opt})$ is given by the eigenvector corresponding to the largest eigenvalue λ_2. A PMF SAR image results from

$$P_{opt} = \bar{E}_{opt}^\dagger G_S \bar{E}_{opt} \qquad (6)$$

where G_S is the Graves power matrix for each pixel of a calibrated image. The application of (6) requires either *a priori* knowledge of G_A and G_B, or they must be estimated directly from the SAR image. For the case when the SAR image features of interest are large in geographical extent consisting of many image pixels (resolution cells) having similar polarimetric characteristics, a representative Graves power matrix can often be successfully estimated from the image yielding favorable contrast enhancement results (*e.g.*

IEEE Geoscience and Remote Sensing Symposium, 1995. IGARSS '95. 'Quantitative Remote Sensing for Science and Applications'., International , Volume: 3 , 10-14 Jul 1995. Page(s): 2244 -2246 vol.3

[5]). However, for the case of geographically localized distributed scatterers consisting of multiple scattering centers having different polarimetric characteristics, the direct use of (4) in the manner described by (5) and (6) is will not typically provide enhancement improvement because the set of polarimetrically diverse scattering centers that together comprise the distributed scatterer are difficult to exploit using a single scattering matrix approach.

Polarimetric Matched Filtering for Distributed Scatterer

The Rayleigh quotient is a powerful representation of polarimetric scattering information, and this ratio of quadratic forms involving Hermitian Graves power matrices is used to establish a foundation for the development of PMF techniques that effectively treat distributed scatterers. For the purposes of this work, a polarimetrically diverse distributed scatterer is taken to consist of a collection of linear orthogonal co-pol (HH and VV) scattering centers arranged in a particular orientation, and the scattering centers are taken to reside in a single resolution cell. The overall physical extent, relative orientation, and polarimetric characteristics of the distributed scatterer are assumed to be approximately known from a scatterer model and/or training measurements. The distributed scatterer is partitioned into subsets of like co-pol resolution cells. The resolution cells that comprise each of these subsets are averaged to estimate a representative scattering matrix, and the corresponding Graves power matrix is determined. The averaging procedure is utilized to account for the relative scattering strength of individual resolution cells within a particular subset, and is representative of the extent to which the corresponding polarization features can be enhanced through the use of a *single* characteristic polarization state. The representative Graves power matrices are denoted G_{HH} and G_{VV}, where the subscripts denote the distributed scatterer's orthogonal co-pol associations. The Rayleigh quotient is formed for each of the orthogonal co-pol power matrices using an estimate of the clutter power matrix G_C obtained from the image. An annihilation approach (Ω is minimized) is taken for the determination of the individual optimum polarization states to avoid polarization impurity effects present in the noisy orthogonal co-pol. The solutions for the individual optimum polarization states $\vec{E}_i^{HH}$ and $\vec{E}_i^{VV}$ are determined from

$$G_{HH}\vec{E}_i^{\min} = \lambda_1 G_C \vec{E}_i^{\min} \Rightarrow \vec{E}_i^{HH} \bullet \vec{E}_i^{\min} = 0 \qquad (7)$$

and

$$G_{VV}\vec{E}_i^{\min} = \lambda_1 G_C \vec{E}_i^{\min} \Rightarrow \vec{E}_i^{VV} \bullet \vec{E}_i^{\min} = 0 \qquad (8)$$

where λ_1 is the smallest eigenvalue, and " $\bullet$ " denotes the vector dot product. The single polarization state that maximizes the distributed scatterer response is formulated as a weighted orthonormal combination of $\vec{E}_i^{HH}$ and $\vec{E}_i^{VV}$ given by

$$\vec{E}_i^{dist} = \frac{w_{HH}\vec{E}_i^{HH} + w_{VV}\vec{E}_i^{VV}}{\left\| w_{HH}\vec{E}_i^{HH} + w_{VV}\vec{E}_i^{VV} \right\|} \qquad (9)$$

where w_{HH} and w_{VV} are determined from the total power in the distributed scatterer's HH and VV resolution cells, respectively. Hence, the single polarization state $\vec{E}_i^{dist}$ ($= \vec{E}_{dist}$) attempts to maximize the total power in the distributed scatterer subject to the appropriate weighting. Analogous to (6), a distributed scatterer PMF SAR image abbreviated (DPMF) results from

$$P_{dist} = \vec{E}_{dist}^{\dagger} G_S \vec{E}_{dist}. \qquad (10)$$

The next section demonstrates the DPMF using simulated SAR data that contains a simulated distributed scatterer and compares the results with the corresponding span image given by

$$P_{span} = \left\{ |S_{HH}|^2 + |S_{VV}|^2 + 2|S_{HV}|^2 \right\}. \qquad (11)$$

Processed Simulated SAR Data and Conclusions

The performance of the DPMF has been investigated using a simulated distributed scatterer constructed from a combination of linear orthogonal co-pol scattering centers. Figure 1 shows the HH-Polarized image detailing the HH response of the simulated distributed scatterer. Similarly, Figure 2 illustrates the VV response. Figure 3 shows the results obtained from applying the basic PMF defined by (6) where the G_A is determined from extracting an average scattering matrix from the resolution cells that contain the distributed scatterer. Figure 4 shows the DPMF result clearly demonstrating successful utilization of polarimetric information. For comparison, the corresponding span image is shown in Figure 5. Note that the SNR performance is included in the figure information. The span performance is not surprisingly similar to the DPMF. The difference between the DPMF image, and the span and PMF images will depend on the polarization characteristics of the distributed scatterer. Note also that the DPMF can be tuned differently for detection versus discrimination by appropriately customizing the weighted combination of the orthogonal co-pol optimum polarization states. Other variations on this theme are also being pursued. The encouraging DPMF performance must be interpreted with reservation until application to actual SAR data. DPMF application (and variants) to actual SAR imagery obtained from NAWC/ERIM P-3 Polarimetric SAR system is underway.

References

[1] W-M. Boerner, W-L. Yan, A-Q. Xi and Y. Yamaguchi, "On the basic principles of radar polarimetry: the target characteristic polarization state theory of Kennaugh,

IEEE Geoscience and Remote Sensing Symposium, 1995. IGARSS '95. 'Quantitative Remote Sensing for Science and Applications'., International , Volume: 3 , 10-14 Jul 1995. Page(s): 2244 -2246 vol.3

Huynen's polarization fork concept, and its extension to the partially polarized case," *Proceedings of the IEEE*, vol. 79, no. 10, pp. 1538-1550, Oct. 1991.
[2] A. B. Kostinski and W-M. Boerner, "On foundations of radar polarimetry," *IEEE Trans. on Antennas and Propagation*, vol. 34, no. 12, pp. 1395-1403, Dec. 1986.
[3] A. B. Kostinski and W-M. Boerner, "On the polarimetric contrast optimization," *IEEE Trans. on Antennas and Propagation*, vol. 35, no. 8, pp. 988-991, Aug. 1987.
[4] R. Courant and D. Hilbert, *Methods of Mathematical Physics*, Vol. I, Wiley, Inc., New York 1953.
[5] J. G. Teti, Jr., F. J. Ilsemann, J. S. Verdi, W.-M. Boerner and S. K. Krasznay, "Application of the polarimetric matched image filter to the assessment of SAR data from the Mississippi flood region," *Proceedings of IGARSS '94*, 8-12 August 1994.

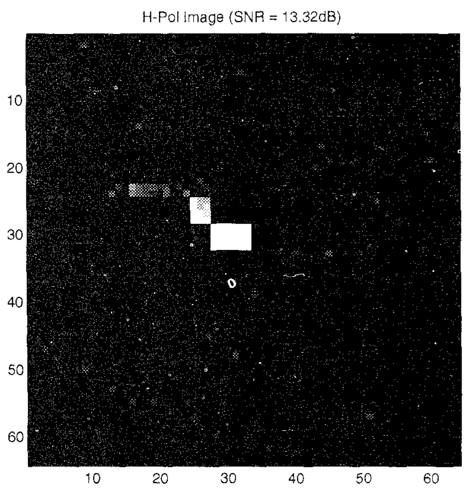

Figure 1: Synthesized SAR *HH*-Polarized image.

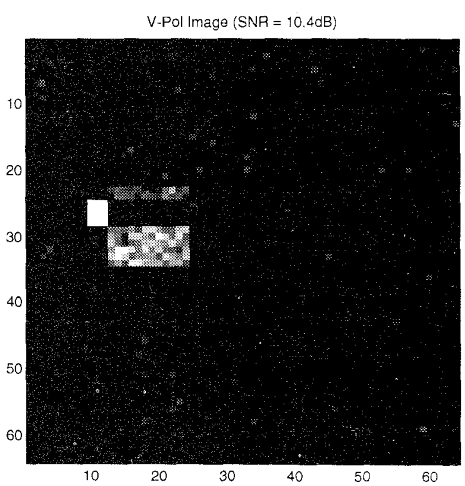

Figure 2: Synthesized SAR *VV*-Polarized image.

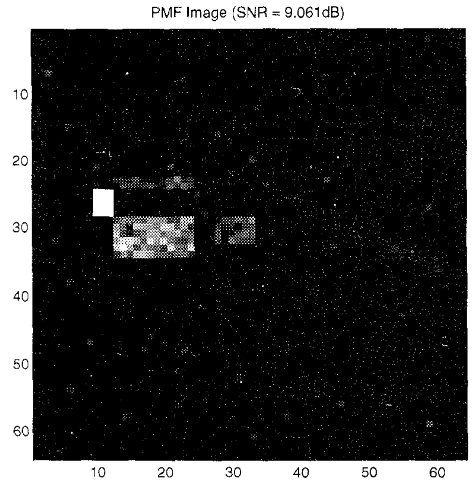

Figure 3: The corresponding point scatterer PMF image.

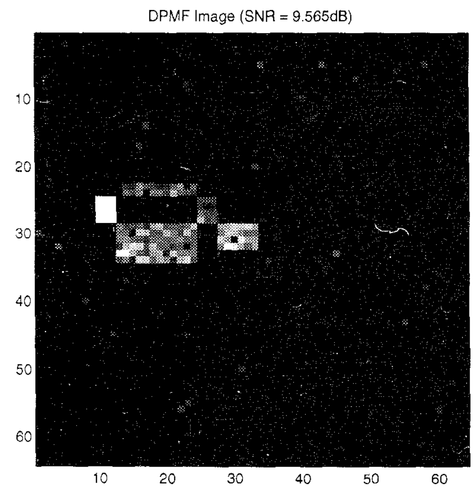

Figure 4: The corresponding DPMF image.

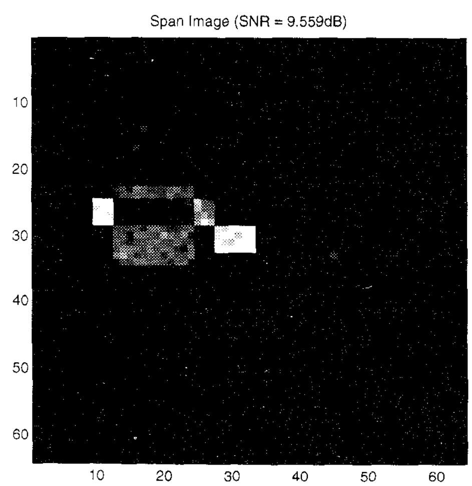

Figure 5: The corresponding span image.

IEEE Geoscience and Remote Sensing Symposium, 1995. IGARSS '95. 'Quantitative Remote Sensing for Science and Applications'., International , Volume: 3 , 10-14 Jul 1995. Page(s): 2244 -2246 vol.3